

Repurposing ubiquitination for innovative antibody conjugation

Hebieshy, A.F. el

Citation

Hebieshy, A. F. el. (2025, October 16). *Repurposing ubiquitination for innovative antibody conjugation*. Retrieved from https://hdl.handle.net/1887/4273517

Version: Publisher's Version

Licence agreement concerning inclusion of doctoral

License: thesis in the Institutional Repository of the University

of Leiden

Downloaded from: https://hdl.handle.net/1887/4273517

Note: To cite this publication please use the final published version (if applicable).



Nanobody ubi-tag conjugates for translation to human dendritic cell targeted antigen delivery

4

This chapter is part of the publication:

A.F. Elhebieshy*, Z. Wijfjes*, et al. Site-directed multivalent conjugation of antibodies to ubiquitinated payloads. Accepted for publication: Nature Biomedical Engineering.



Nanobody ubi-tag conjugates for translation to human dendritic cell targeted antigen delivery

Angela F. el Hebieshy, Zacharias Wijfjes, Camille M. Le Gall, Jim Middelburg, Kim E. de Roode, Felix L. Fennemann, Marjolein Sluijter, Thorbald van Hall, Douwe J. Dijkstra, Leendert A. Trouw, Floris J. van Dalen, Andrea Rodgers Furones, Johan M. S. van der Schoot, Ian Derksen, Hans de Haard, Bas van der Woning, Cami M. P. Talavera Ormeño, Bjorn R. van Doodewaerd, Carl G. Figdor, Gerbrand J. van der Heden van Noort, Paul W.H.I. Parren, Sandra Heskamp, Huib Ovaa, Martijn Verdoes, Ferenc A. Scheeren.

Abstract

Nanobodies, also known as sdAbs or VHHs, hold great potential for the development of dendritic cell (DC)-targeted vaccines due to their small size, high specificity, and ability to penetrate tissues efficiently. In this study, we demonstrate that ubi-tagged VHHs retain their functionality, with the ubi-tag not interfering with VHH antigen binding. Furthermore, we show that the ubi-tag serves as a conjugation tag and also enhances the solubility of the attached peptide, acting as an effective solubility enhancer for hydrophobic epitopes. We then generated an anti-DC-SIGN VHH-Ub₂-gp100_p conjugate and demonstrate its functionality *in vitro*, showcasing the potential of ubitagged VHH-peptide epitope conjugates as a vehicle for DC-targeted vaccines in a human setting.

Introduction

Nanobodies, or single-domain antibody fragments, are derived from unique heavy-chain-only antibodies found in camelids. Unlike conventional antibodies, which consist of two heavy and two light chains, nanobodies consist solely of the variable heavy-chain domain (VHH), which is responsible for antigen recognition.¹ Despite their small size (approximately 15 kDa), nanobodies maintain antigen-binding capacities comparable to full-sized antibodies, making them highly versatile in biomedical applications¹. Their small size, superior stability, high specificity, and ability to penetrate tissues efficiently, contribute to their effectiveness in both therapeutic and diagnostic applications. For this reason, nanobodies are also attractive to use for the development of dendritic cell (DC)-targeted vaccines, which aim to enhance immune responses against infectious diseases, cancer, and other conditions²-5.

Nanobodies targeting DC cell surface receptors, such as CLEC9A and CD11c, and DC-SIGN, enable targeted delivery of antigens to DCs ^{3,6,7}. Since VHHs are predominantly produced via recombinant expression in bacterial systems, one approach for generating VHH-peptide epitope conjugates involves recombinant DNA. In this technique, the coding DNA sequences of the VHH and peptide epitopes are linked together within a recombinant plasmid, enabling the co-expression of a single polypeptide chain comprising both the VHH and the peptide epitope. This method facilitates the

production of a bifunctional protein, where the VHH domain and the epitope are expressed in one genetically encoded fusion product, allowing for efficient synthesis in bacterial hosts. While this approach seems straightforward, it often presents challenges due to the hydrophobic nature of antigenic peptides ⁸, leading to low expression and improper folding of the resulting fusion proteins. This limits the wide application of bacterial expression for producing VHH-peptide conjugates.

An alternative approach is sortagging, where a VHH is produced with a sortag motif at its C-terminus and then chemoenzymatically conjugated to a chemically synthesized peptide epitope with a polyglycine motif at its N-terminus⁹. Chemical synthesis of the peptide epitope provides more flexibility to attach chemical moieties to enhance the solubility compared to genetic fusions. For instance, the solubility of the highly hydrophobic peptide NY-ESO-1 was improved by chemically attaching polyethylene glycol (PEG) to it.⁹

Ubiquitin has also been shown to enhance the solubility and promote the proper folding of proteins when used as a fusion tag ¹⁰. Encouraged by our data in Chapter 3, where we observed strong T cell activation with ubi-tagged Fab-peptide conjugates, we sought to apply ubi-tag conjugation to generate VHH-peptide epitope conjugates. Our aim was to investigate the impact of the presence of a ubi-tag on the solubility of antigenic peptides, assess the feasibility of ubi-tag conjugation for VHHs, and translate the previously observed effects of the ubi-tagged conjugates for DC-targeted antigen delivery to human applications.

Results

To explore the applicability of ubi-tagging for DC-targeted antigen delivery, we broadened the scope towards nanobody (VHH)-conjugates (Fig. 1a). The high stability, solubility, and ease of production of nanobodies have raised interest in the use of these small-sized (15 kDa) targeting moieties¹. We produced two ubi-tagged VHHs (VHH-Ub(K48R)^{don}), one targeting hDC-SIGN (CD209)¹¹ and the other targeting ALFA-tag¹² as a non-targeted control (ntVHH-Ub) (Fig. 1b and Supplementary Fig. S1 and S4, and Supplementary Table S1). As the size of the ubi-tag (16 kDa) is roughly equal to the size of the nanobody, we first verified that ubi-tagging does not hinder target binding. We performed a binding assay on DC-SIGN transfected CHO cells and DC-SIGN expressing monocyte-derived DCs (moDCs) (Fig. 1c and Supplementary Fig. S2). The results revealed a pronounced, DC-SIGN expression- and dose-dependent enhancement in the fluorescent signal for the DC-SIGN targeted Rho-Ub₂-VHH conjugate. In contrast, no such increase was observed for the Rho-Ub₂-ntVHH.

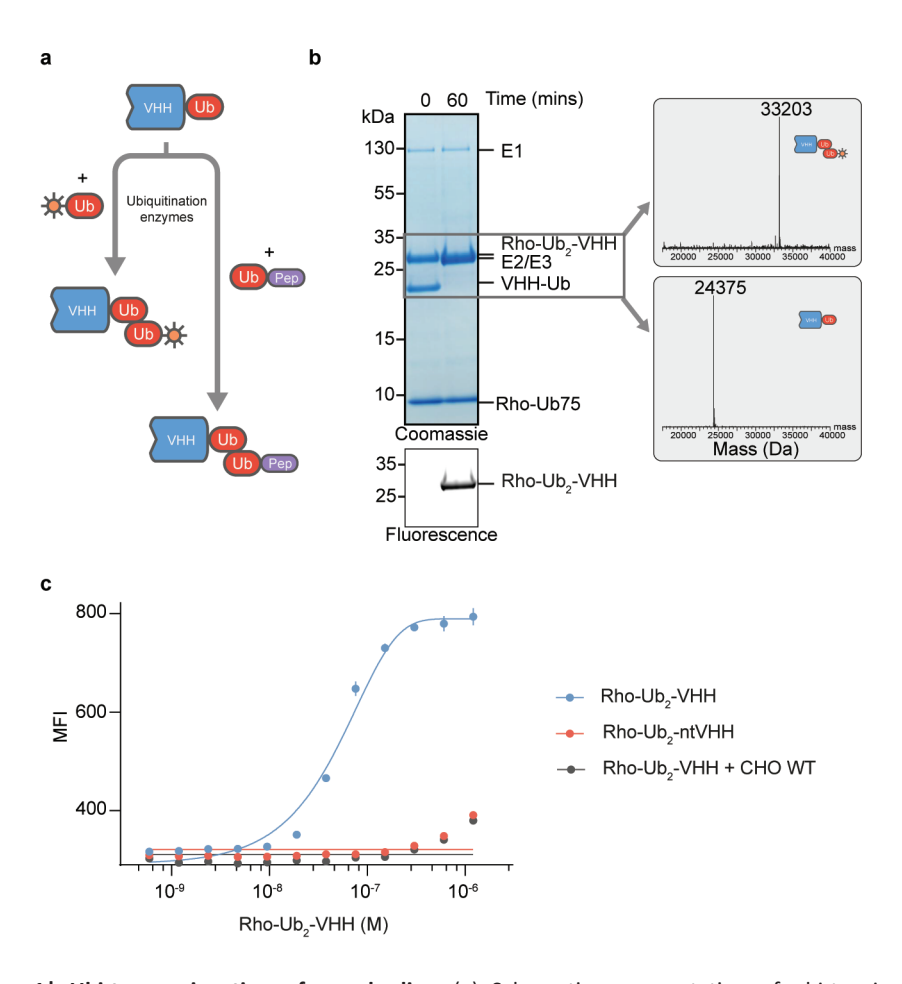


Figure 1| **Ubi-tag conjugation of nanobodies.** (a) Schematic representation of ubi-tagging for nanobodies. (b) Non-reducing (fluorescent) SDS-PAGE analysis and deconvoluted ESI-TOF mass spectra of formation of Rho-Ub₂-VHH through ubi-tagging of VHH-Ub^{don} and Rho-Ub^{acc}. (c) Binding assay on DC-SIGN transfected CHO cells with DC-SIGN targeted Rho-Ub₂-VHH (blue), ALFAtag targeted Rho-Ub₂-ntVHH (red), and DC-SIGN targeted Rho-Ub₂-VHH on WT CHO cells (black). Data are shown as MFI of Rhodamine-channel and a curve fit (Sigmoidal, 4PL, X = log(conc.)) on data points (n = 2).

In the field of targeted antigenic peptide delivery the hydrophobicity of CD8-epitopes is a prevalent problem⁸. We reasoned that since ubiquitin is well-known for its high solubility and stability, the fusion of a ubi-tag to hydrophobic peptides could enhance their solubility¹⁰. To demonstrate this, we generated a library of VHH-Ub₂-peptide conjugates, including hydrophobic peptides known to be challenging to ligate to antibodies, nanobodies or chemokines using other techniques^{8,9}. All tested Ub-peptide fusions were readily synthesized and conjugated to VHH-Ub(K48R)^{don} without solubility issues (Fig. 2a and Supplementary Fig. S5).

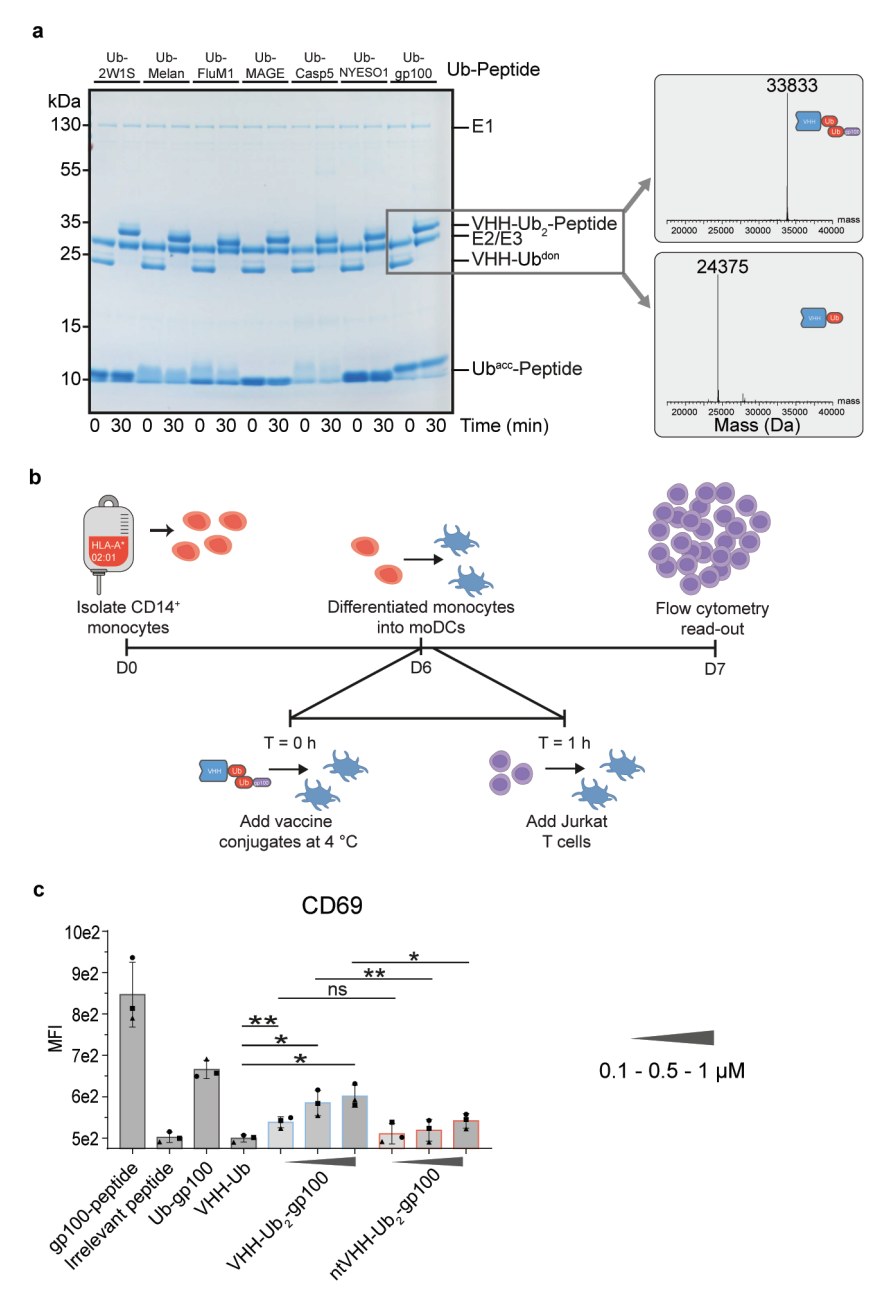


Figure 2 | Generation and validation of VHH-Ub $_2$ -antigenic peptide conjugates. (a) SDS-PAGE analysis of VHH-Ub $_2$ -antigenic peptide conjugates and deconvoluted ESI-TOF mass spectra of VHH-Ub $_2$ -gp100 $_p$. VHH-Ub $_2$ -ontigenic peptide to respectively Ub $_2$ -EAWGALANWAVDSA (2W1S), Ub $_2$ -ELAGIGILTV (Melan), Ub $_2$ -GILGFVFTL (FluM1), Ub $_2$ -CKVLEYVIKV (MAGE), Ub $_2$ -FLIIWQNTM (Casp5), Ub $_2$ -CLMWITQV (NYESO1) and Ub $_2$ -CYLEPGPVTA (gp100). (b) Schematic illustration of reporter Jurkat T cell activation assay. In short, moDCs were generated, pulsed (1 h., 4 °C) with vaccine conjugate (VHH-Ub $_2$ -gp100p) or non-targeting control (ntVHH-Ub $_2$ -gp100p), and washed. Subsequently, reporter Jurkat T

cells were added in 1:5 ratio and incubated overnight followed by flow cytometry analysis. (c) Flow cytometry analysis of CD69 expression. Data (N=3) are shown as mean ±SD, paired T tests, **P<0.01, *P<0.05, ns P>0.05.

Glycoprotein 100 (gp100) is considered a melanoma tumor-associated antigen of which gp100 $_{280\cdot288}$ (gp100 $_{\rm p}$) has been identified as an HLA-A*0201 binding epitope¹³. We therefore proceeded to examine the functionality of the human DC targeted anti-DC-SIGN VHH-Ub $_{\rm 2}$ -gp100 $_{\rm p}$ by pulsing moDCs and subsequent incubation with reporter Jurkat T cells recognizing the MHC I-gp100 $_{\rm p}$ epitope complex¹⁴. Activation of the Jurkat T cells was assessed by CD69 expression the next day and indicated that the VHH-Ub $_{\rm 2}$ -gp100 $_{\rm p}$ led to antigen presentation of the gp100 epitope by moDCs in a dose-dependent fashion (Fig. 2b,c). Significant differences were observed between the DC-SIGN targeted VHH-Ub $_{\rm 2}$ -gp100 $_{\rm p}$ and non-targeted variant, which demonstrates the potentiating effect of receptor-mediated antigen uptake¹⁵.

In a more physiologically relevant setting, we transfected primary CD8⁺ T cells from HLA-A*02:01⁺ donors with a gp100 $_p$ specific T cell receptor (TCR) (Supplementary Fig. S3) to assess the efficacy of the VHH-Ub $_2$ -gp100 $_p$ to induce HLA-A*02:01⁺ moDC-mediated activation of primary human T cells (Fig. 3a)¹⁵. Proliferation (Fig. 3b), activation (Fig. 3c,d) and cytokine secretion (Fig. 3e) of the T cells were assessed and showed a more potent dose-dependent increase in the conditions where moDCs were pulsed with anti-DC-SIGN VHH-Ub $_2$ -gp100 $_p$ compared to the non-targeted conjugate, indicating the potential of nanobody-peptide epitope conjugates for the development of DC-targeting vaccines in a human setting.

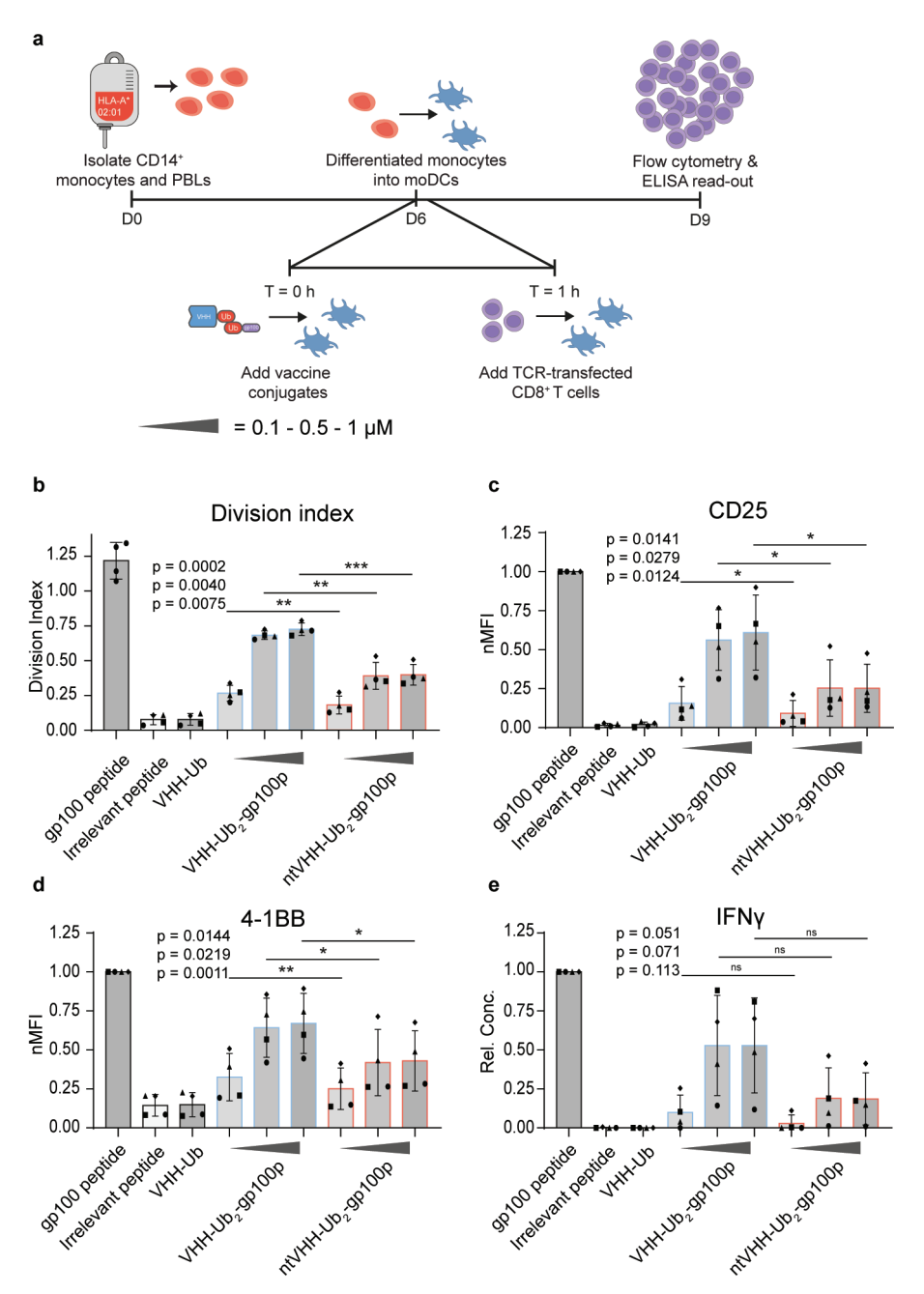


Figure 3 | Primary TCR-transfected CD8+ T cell activation assay for the validation of VHH-Ub₂-gp100_p. (a) Schematic representation of primary TCR-transfected CD8+ T cell activation assay. HLA-A*02:01+ moDCs were generated and pulsed with 0.1-0.5-1 μ M vaccine conjugate or 1 μ M control condition for 1 h. at 37 °C. TCR transfected CD8+ T cells were added in 1:5 ratio and after 3 days, supernatant and cells were harvested for analysis. Transfection efficiency is shown in Supplementary Fig. S3. (b-d) flow cytometry analysis of CD8+ T cells. Division index was calculated for different conditions based on

CTV signal (b). Data (n = 4) are shown as mean \pm SD normalized to positive control (gp100 peptide) for CD25 (c), and 4-1BB (d). Paired T tests, ***P<0.001, **P<0.01, *P<0.05, ns P>0.05. (e) ELISA analysis (n = 4) for IFN γ . Data are shown as mean \pm SD normalized to positive control. Paired T tests, p-values are noted in figure.

Discussion

In this work, we broadened the scope of ubi-tagging towards nanobody (VHH)conjugates for human DC-targeted antigen delivery. First, we showed that although ubi-tag conjugation would significantly add to the molecular weight of the conjugate, considering the size of a VHH of 15 kDa and the di-ubiquitin formed during ubi-tag conjugation around 16 kDa, it does not hinder the binding of VHH towards its target. This could be of additional benefit in therapeutic or diagnostic applications, as the increase in molecular weight will contribute to an extended half-life of the VHH and thereby enhance their efficacy¹⁶. Next, we proceeded to demonstrate that ubi-tagging improves the solubility of nanobody-antigen conjugates for a library of notoriously insoluble epitopes^{8,9}. Ubiquitin is one of the most stable and soluble proteins in eukaryotes. Owing to these exceptional physicochemical properties, it is often used as a solubility tag to enhance the solubility and expression yield of fused proteins in bacterial expression systems by chaperoning for correct folding and reducing the chances of protein aggregation during expression¹⁰. With this in mind, we successfully attempted to enhance the solubility of antigenic epitopes known for their extremely poor solubility by chemically synthesizing these peptides fused to the C-terminus of an acceptor ubi-tag. After successfully synthesizing and purifying these ubi-tag fused peptides, we proceeded to conjugated them to a ubi-tagged VHH with a high reaction efficiency, approaching completion in 30 minutes. Next, we validated the functionality of the generated anti-DC-SIGN VHH-Ub₂-gp100₀ as a human DC-targeting vaccine in a reporter Jurkat T cell activation assay and a primary TCR-transfected CD8+ T cell activation assay. In both assays, significant differences were observed in the results of the DC SIGN targeted VHH-Ub₂-gp100_n compared to the non-targeted variant, and a potent dose-dependent T cell activation was observed. The results obtained indicate that ubi-tagging enhances the solubility of hydrophobic epitopes, and demonstrate that it is feasible on nanobodies and that ubi-tagged nanobody-peptide epitope conjugates are of interest to be further examined as DC-targeted vaccine vehicles in a human setting.

Methods

General cell culture conditions

Jurkat T cells were cultured in T75 flasks in RPMI 1640 medium (ThermoFischer) supplemented with heat inactivated fetal bovine serum (10%, Greiner Bio-One), L-glutamine (4 mM, Gibco), non-essential amino acids (NEM) (1 mM, Gibco) and

Antibiotic-Antimycotic (1%, Gibco). Cells were maintained at 37 $^{\circ}$ C and 5% CO $_{2}$, routinely examined by morphology analysis and tested for mycoplasma.

Solid-phase peptide synthesis

Solid-phase peptide synthesis (SPPS) of Rho-Ub and Ub-peptides was performed on a Syro II Multisyntech Automated Peptide synthesizer (SYRO robot; Part Nr: S002PS002; MultiSyntech GmbH, Germany) on a 25 μ mol scale using standard 9-fluorenylmethoxycarbonyl (Fmoc) based solid phase peptide chemistry. Both Ub variants were synthesized based on the procedure described by El Oualid *et al.*¹⁷ using a fourfold excess of amino acids relative to pre-loaded Fmoc amino acid trityl resin (between 0.17 and 0.20 mmol/g, Rapp Polymere, Germany). Ub-peptides were prepared as a linear synthesis, where the peptides listed below were synthesized attached to the C-terminus of Ub. To prepare Rho-Ub, 5-carboxyrhodamine110 (Rho) was coupled to the N-terminus of Ub following SPPS as described by Geurink *et al*¹⁸. All synthetic products were purified by RP-HPLC on a Waters preparative RP-HPLC system equipped with a Waters C18-Xbridge 5 μ m OBD (10 x 150 mm) column. The purified products were lyophilized and assayed for purity by high resolution mass spectrometry on a Waters Acquity H-class UPLC with XEVO-G2 XS Q-TOF mass spectrometer and by SDS-PAGE analysis.

Peptide	Peptide sequence
2W1S	EAWGALANWAVDSA
Melan-A _{26–35,A27L}	ELAGIGILTV
FluM ₁₅₈₋₆₆	GILGFVFTL
MAGE-A1 ₂₇₈₋₂₈₆	KVLEYVIKV
Caspase ₅₆₇₋₇₅	FLIIWQNTM
NY-ESO-1 ₁₅₇₋₁₆₅ , C165Abu	SLLMWITQAbu
gp100 ₂₈₀₋₂₈₈	YLEPGPVTA

Mass spectrometry

Mass spectrometry analysis was carried out on Waters ACQUITY UPLC-MS system equipped with a Waters ACQUITY Quaternary Solvent Manager (QSM), Waters ACQUITY FTN AutoSampler, Waters ACQUITY UPLC Protein BEH C4 Column (300 Å, $1.7 \mu m$, $2.1 \times 50 \text{ mm}$) and XEVO-G2 XS QTOF Mass Spectrometer (m/z = 200-2500) in ES+ mode. Sample were run using 2 mobile phases: A = 1% MeCN, 0.1% formic acid in water and B = 1% water and 0.1% formic acid in MeCN with a runtime of 14 minutes. In the first 4 minutes, salts and buffer components were flushed from LC column using 98% A and 2% B. In the next 7.5 minutes, a gradient of 2-100% B was used, followed by 0.5 minutes of 100% B and subsequent reduction to 2% B and 98% A in 2 minutes. Data processing

was performed using Waters MassLynx Mass Spectrometry Software 4.1, where the mass was obtained by deconvolution with the MaxEnt1 function.

Protein expression and purification

The E1 ubiquitin-activating enzyme UBE1 carrying an N-terminal His-tag was expressed from a pET3a vector in E. coli BL21(DE3) in autoinduction media for 2-3 hours at 37 °C, after which the bacteria were allowed to grow overnight at 18 °C. Next, bacteria were harvested and lysed by sonication, followed by His-affinity purification using Talon metal affinity resin (Clontech Inc., Palo Alto, CA, USA). Subsequently, the protein was further purified by anion exchange using a Resource Q column (GE Healthcare), followed by size exclusion using a Superdex 200 column (GE Healthcare).

The E2/E3 enzyme chimera plasmid was obtained as a gift from dr. Vincent Chau (Penn State, USA). The expression plasmid consists of the RING domain of the E3 ubiquitin ligating enzyme gp78 fused to the N-terminus of the E2 ubiquitin-conjugating enzyme Ube2g2 in a PET28a-TEV vector.

The E2/E3 enzyme chimera was expressed and purified as described¹⁹. In brief, the fusion protein was expressed in E. coli BL21(DE3) cells grown in LB at 37°C until OD₆₀₀ = 0.4-0.6 and induced with 0.4 mM IPTG for 4 hours at 30 °C. The harvested cells were lysed with Bugbuster protein extraction reagent (Millipore) according to manufacturer's protocol. The fusion protein was purified on Ni-NTA resin followed by size exclusion using a Superdex 200 column (GE Healthcare). Next, TEV protease cleavage was carried out overnight, and the cleaved fusion protein was further purified using a Resource Q column (GE Healthcare).

Sequences for the different VHH-ubiquitin fusions were cloned in the Pet30b vector and expressed in Rosetta-gami™ 2 (DE3) grown in LB medium at 37 °C until an OD₆₀₀ of 0.5 was reached and induced with 1 mM IPTG for 18 hours at 20 °C. Next, the bacteria were harvested and lysed by sonication followed by Ni-NTA purification. Subsequently, TEV protease cleavage was carried out to cleave the N-terminal his-tag and the cleaved VHH-Ub was further purified by size exclusion chromatography using a Superdex 200 column (GE Healthcare).

Ubi-tag conjugation reaction

Ubi-tag conjugation reactions were carried out in the presence of 0.25 μ M E1 enzyme, 20 μ M E2/E3 hybrid enzyme, 10 mM MgCl₂, and 5 mM ATP in PBS. For analysis of the reaction efficiency by SDS-PAGE, an initial reaction sample was taken from the reaction mixture prior to the addition of ATP. After the addition of ATP, the reaction was incubated at 37°C for 30 minutes while shaking. Conjugation reaction samples were analyzed by quenching 2-5 μ L of the reaction mixture in sample buffer supplemented with β -mercaptoethanol, boiled for 15 minutes at 95°C and run on 12% Bis-Tris gels (Invitrogen) by SDS-PAGE with MOPS as running buffer. Gels were stained using InstantBlue Coomassie Protein

Stain (abcam) and imaged using Amersham600. Fluorescently labeled proteins were visualized by in-gel fluorescence using Typhoon FLA 9500 imaging system (GE Life Sciences) prior to staining with Coomassie. Small-scale reactions were carried out on a scale corresponding to 2.5 μ g VHH-Ub while large-scale reactions were carried out on a 200 μ g to 1 mg scale. For the purification of ubi-tagged VHH conjugates from the reaction mixture, 100 μ L HisPurTM Ni-NTA Resin was added to the completed reaction mixture and incubated for 15 mins at 4 °C to capture the his-tagged E1 and E2/E3 enzyme, followed by centrifugation. The supernatant containing the Ubi-tagged VHH conjugates was further purified using size exclusion chromatography using a Superdex 200 column (GE Healthcare).

Binding study VHH-Ub,-Rho

CHO cells transfected with DC-SIGN, WT CHO cells or day 6 moDCs (GM-CSF, IL-4) were harvested and plated at 30,000 cells per well. VHH-Ub₂-Rho was added in a dilution series to the cells and the cells were incubated (30 min., 4 °C). Cells were washed and fluorescence on alive cells was measured using a FACSVerseTM (BD Biosciences).

Jurkat T cell activation assay

moDCs from HLA-A*02:01 donors prepared as described below were harvested and plated at 10,000 cells per condition. moDCs were pulsed (0.5 h., 4 °C) with vaccine conjugates at 0.1, 0.5 or 1 μ M. After the incubation, Jurkat T cells²⁰ (50,000, 1:5 ration) were added and the co-culture was incubated (1 d., 37 °C). The cells were spun down (1700 rpm., 2 min., 4 °C) and the cells were analyzed using a FACSVerseTM (BD Biosciences).

Primary TCR-transfected T cell activation assay

Donor-matched PBLs were thawed and CD8⁺T cells were isolated using magnetic-assisted cell sorting according to manufacturer's protocol (CD8⁺ T cell Isolation Kit, human, Miltenyi Biotec). T cells were mRNA-transfected by electroporation with a TCR recognizing the gp100₂₈₀₋₂₈₈ epitope (YLEPGPVTA)²¹. Afterwards, cells were recovered in X-VIVO, phenol free (Lonza) supplemented with 5% human serum. In tandem, moDCs from HLA-A*02:01 donors prepared as described below were harvested and plated at 10,000 cells per condition. moDCs were pulsed (1 h., 37 °C) with vaccine conjugates at 0.1, 0.5 or 1 μM. In tandem, transfected CD8⁺ T cells were stained with CellTraceTM Violet (ThermoFischer) for 20 min. at 37 °C and recovered in X-VIVO supplemented with 2% human serum. Then, moDCs were washed and transfected CD8⁺ T cells (50,000) were added. The moDC-CD8 T cell coculture was incubated (3 d., 37 °C). The cells were spun down (1700 rpm., 2 min., 4 °C), supernatant was stored for ELISA analysis, and the cells were analyzed using a FACSVerseTM (BD Biosciences).

moDCs generation

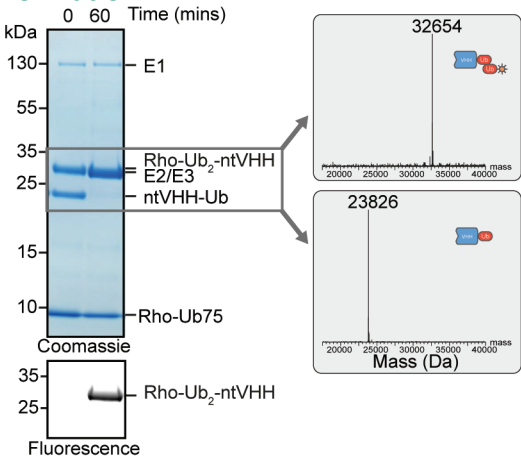
Buffy coats were obtained from Sanquin (Nijmegen, The Netherlands) and diluted to 200 mL with PBS supplemented with 2 mM EDTA. The suspension was divided over conical 5 x 50 mL tubes and 10 mL of Lymphoprep (07851, Stemcell) was added below. Cells were spun (20 min., rt, 2100 rpm., brake (3,1)). Afterwards, PBMCs were collected and washed with wash buffer (1% human serum, 2 mM EDTA in PBS) until supernatant was clear. Then ACK lysis was performed by adding 5 mL ACK buffer (150 mM NH₄Cl, 10 mM KHCO₃, 0.1 mM EDTA, pH=7.4) for 5 min. at room temperature. Afterwards cells were washed with PBS and CD14⁺ monocytes were isolated using magnetic-assisted cell sorting according to manufacturer's protocol (CD14 MicroBeads UltraPure, human, Miltenyi Biotec). Flowthrough PBLs were stored, while CD14⁺ monocytes were seeded at 8-12e6 cells per T75 flask in 10 mL X-VIVO (Lonza) supplemented with 2% human serum, 300 U/mL IL-4, and 450 U/mL GM-CSF. At day 3, medium was refreshed. At day 6, moDCs were harvested and used in experiments.

ELISA

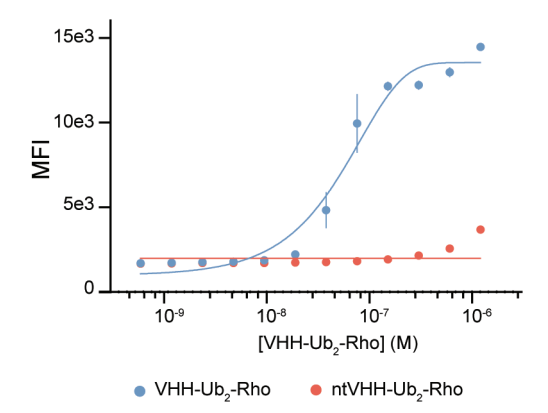
Supernatant was stored at -20 $^{\circ}$ C and thawed for ELISA analysis. Manufacturer's protocol was followed for hIFN $_{\gamma}$ (IFN gamma Uncoated ELISA kit, Invitrogen). Flow cytometry and antibodies

For FACS analysis, cells were washed with PBS, followed by life/death staining (20 min., rt) in 50 μL eBioscience™ Fixable Viability Dye eFluor™ 780 (1:2000, ThermoFischer). Cells were washed once with PBA and antibody mixes were added (30 min., 4 °C). Cells were washed twice with PBA, taken up in 100 μL PBA and FACS analyses were performed on a FACSLyric™ (BD Biosciences) or a FACSVerse™ (BD Biosciences). The following antibodies were used for staining: hCD8 (1:20 dil., APC, clone RPA-T8, BD Biosciences), hCD25 (1:50 dil., PE/Cy7, clone BC96, BioLegend), hCD69 (1:20 dil., PerCP, clone L78, BD Biosciences), h4-1BB (1:20 dil., PE, clone 4B4-1, BD Pharmingen).



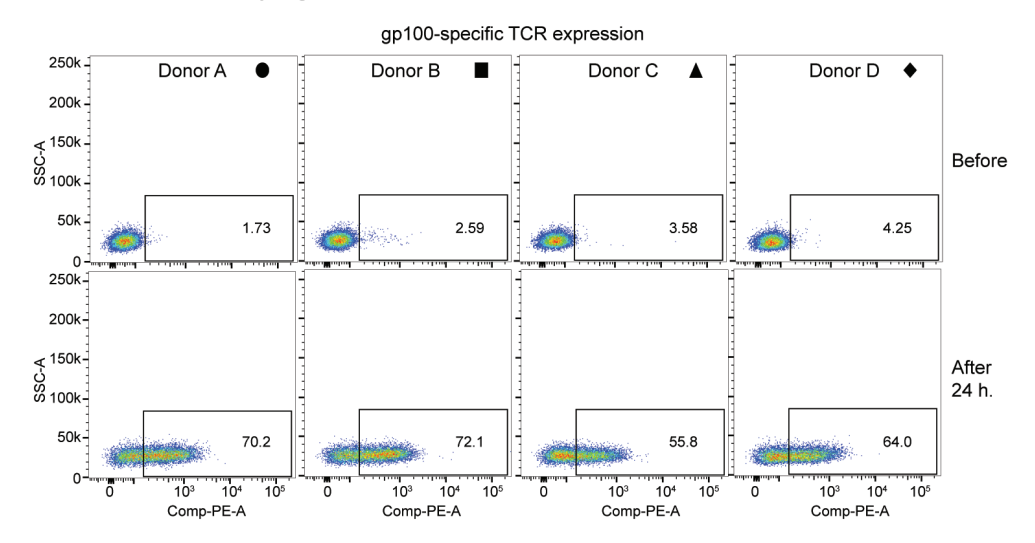


S1 Conjugation of ntVHH-Ub^{don} **to or Rho-Ub**^{acc}. SDS-PAGE analysis visualized by Coomassie Blue staining. The generated Rho-Ub₂-ntVHH was isolated from the reaction mixture and its purity assessed using ESI-TOF mass spectrometry.

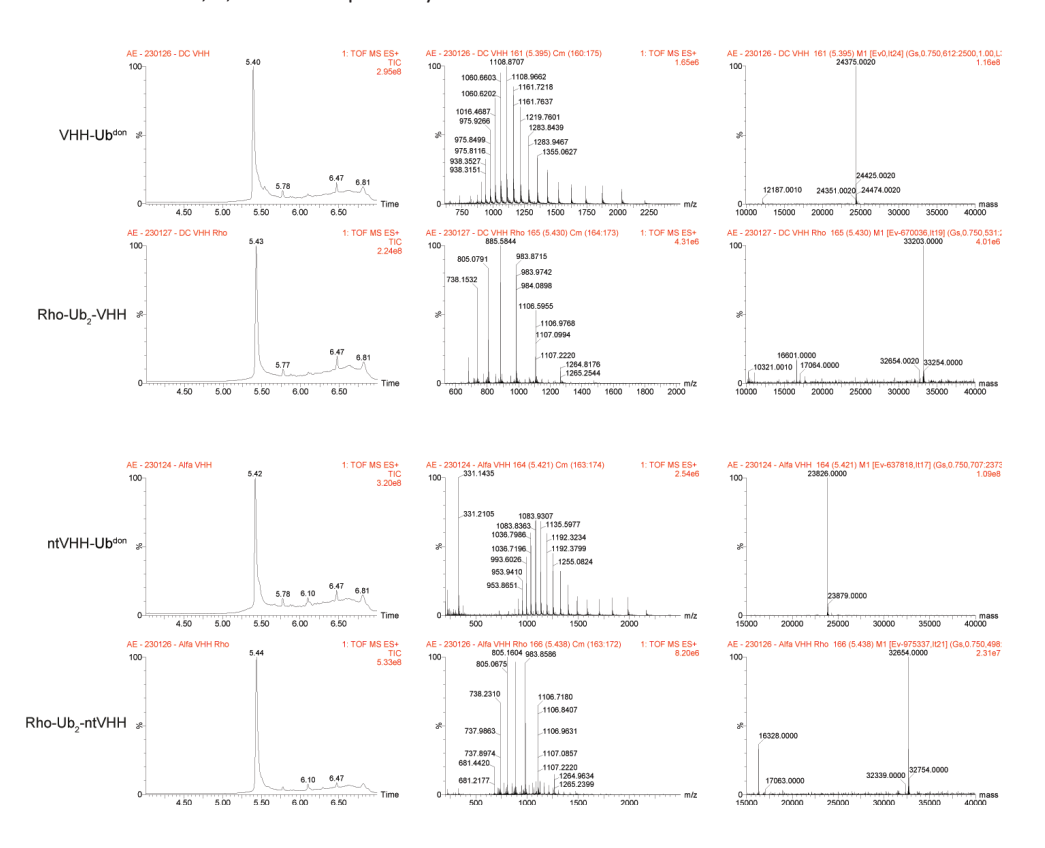


S2 Binding assay of VHH-Ub₂-Rho on moDCs. moDCs were incubated (30 min., 4 °C) with rhodamine-labed anti-DC-SIGN VHH (VHH-Ub₂-Rho) or anti-ALFAtag VHH (ntVHH-Ub₂-Rho). Fluorescence was assessed using flow cytometry. Data (N=3) are shown as mean \pm SD with a curve fit (Sigmoidal, 4PL, X = log(conc.)).

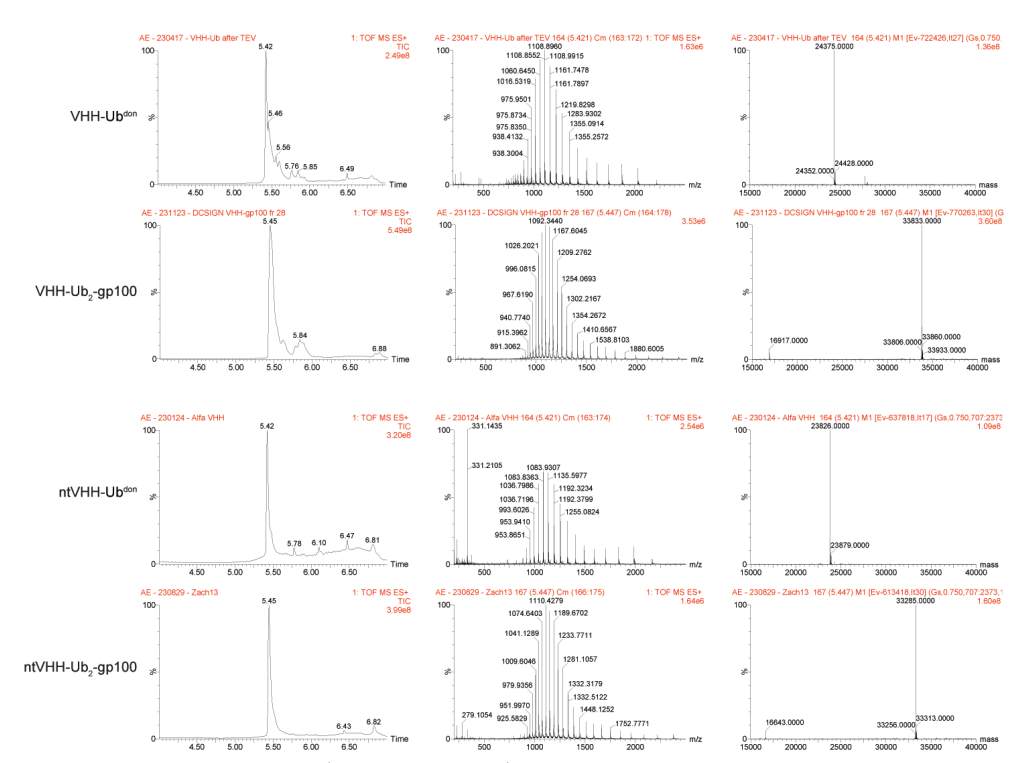
Transfection efficiency Fig 3a



S3 Transfection efficiency of TCR on primary CD8⁺ T cells after 24 h. Transfection efficiency of TCR was analyzed by dextramer staining. After 24 h. transfection effeciencies were 68.5%, 69.5%, 52.2% and 59.8% for donor A, B, C and D respectively.



S4 LC-MS analysis of VHH-Ub^{don} and ntVHH-Ub^{don} conjugation to Rho-Ub^{acc} forming Rho-Ub₂-VHH and Rho-Ub₂-ntVHH, respectively. Total ion chromatograms (left), ESI-TOF spectra (middle) and deconvoluted ESI-TOF mass spectra (right).



S5 LC-MS analysis of VHH-Ub don and ntVHH-Ub don conjugation to Ub acc -gp100p forming VHH-Ub $_2$ -gp100p and ntVHH-Ub $_2$ -gp100p, respectively. Total ion chromatograms (left), ESI-TOF spectra (middle) and deconvoluted ESI-TOF mass spectra (right).

Table S1 VHH-Ub^{don} **sequences.** Table displays protein sequences of VHH-Ub^{don} used. The N-terminal His-tag can be removed by TEV-protease to obtain the VHH-linker-ubiquitin construct. The sequence for the anti-DC-SIGN VHH was obtained in house, whereas the sequence for the anti-ALFAtag VHH was obtained from literature.

	Sequence
His-tag + TEV	MGSSHHHHHHHHHSSGENLYFQG
anti-DC-SIGN-VHH	MQVQLVESGGGLVQAGGSLRLSCVVSGRTFNLYPMGWFRQTPGKEREFVAA LSQDGLSKDYADSNGLSKDYADPVKGRFTISGDNAKHTLYLHMNSLEPDDTAV YYCASGSLLRPVSRSRTDYGYWGQGTQVTVSS
Linker-Ub ^{don}	GGGGSGGGGGGGSMQIFVKTLTGKTITLEVEPSDTIENVKAKIQDKEGIPP DQQRLIFAGRQLEDGRTLSDYNIQKESTLHLVLRLRGG*
His-tag + TEV	MGSSHHHHHHHHHSSGENLYFQG

anti-ALFAtag-VHH	MGSGDASDSEVQLQESGGGLVQPGGSLRLSCTASGVTISALNAMAMGW YRQAPGERRVMVAAVSERGNAMYRESVQGRFTVTRDFTNKMVSLQMD NLKPEDTAVYYCHVLEDRVDSFHDYWGQGTQVTVSS
Linker-Ub ^{don}	GGGGSGGGGGGGSMQIFVKTLTGKTITLEVEPSDTIENVKAKIQDKEGI PPDQQRLIFAGRQLEDGRTLSDYNIQKESTLHLVLRLRGG*

References

- 1. Verhaar, E. R., Woodham, A. W. & Ploegh, H. L. Nanobodies in cancer. *Semin Immunol* **52**, (2021).
- 2. Fang, T. *et al.* Targeted antigen delivery by an anti-class II MHC VHH elicits focused αMUC1(Tn) immunity. *Chem Sci* **8**, 5591–5597 (2017).
- 3. Pishesha, N. *et al.* Induction of antigen-specific tolerance by nanobody—antigen adducts that target class-II major histocompatibility complexes. *Nature Biomedical Engineering 2021 5:11* **5**, 1389–1401 (2021).
- 4. Duarte, J. N. *et al.* Generation of Immunity against Pathogens via Single-Domain Antibody-Antigen Constructs. *J Immunol* **197**, 4838–4847 (2016).
- 5. Woodham, A. W. *et al.* Nanobody-Antigen Conjugates Elicit HPV-Specific Antitumor Immune Responses. *Cancer Immunol Res* **6**, 870–880 (2018).
- 6. Cauwels, A. *et al.* Delivering type i interferon to dendritic cells empowers tumor eradication and immune combination treatments. *Cancer Res* **78**, 463–474 (2018).
- 7. Cauwels, A. *et al.* Targeting interferon activity to dendritic cells enables in vivo tolerization and protection against EAE in mice. *J Autoimmun* **97**, 70–76 (2019).
- 8. Chowell, D. *et al.* TCR contact residue hydrophobicity is a hallmark of immunogenic CD8+ T cell epitopes. *Proc Natl Acad Sci U S A* **112**, E1754–E1762 (2015).
- 9. Le Gall, C. *et al.* Efficient targeting of NY-ESO-1 tumor antigen to human cDC1s by lymphotactin results in cross-presentation and antigen-specific T cell expansion. *J Immunother Cancer* **10**, (2022).
- 10. Roscoe, B. P., Thayer, K. M., Zeldovich, K. B., Fushman, D. & Bolon, D. N. A. Analyses of the effects of all ubiquitin point mutants on yeast growth rate. *J Mol Biol* **425**, 1363–1377 (2013).
- 11. Geijtenbeek, T. B. H. *et al.* Identification of DC-SIGN, a novel dendritic cell-specific ICAM-3 receptor that supports primary immune responses. *Cell* **100**, 575–585 (2000).
- 12. Götzke, H. *et al.* The ALFA-tag is a highly versatile tool for nanobody-based bioscience applications. *Nat Commun* **10**, (2019).
- 13. Cox, A. L. *et al.* Identification of a peptide recognized by five melanoma-specific human cytotoxic T cell lines. *Science* **264**, 716–719 (1994).

- 14. Schaft, N., Lankiewicz, B., Gratama, J. W., Bolhuis, R. L. H. & Debets, R. Flexible and sensitive method to functionally validate tumor-specific receptors via activation of NFAT. *J Immunol Methods* **280**, 13–24 (2003).
- 15. Wijfjes, Z., van Dalen, F. J., Le Gall, C. M. & Verdoes, M. Controlling Antigen Fate in Therapeutic Cancer Vaccines by Targeting Dendritic Cell Receptors. *Mol Pharm* **20**, 4826–4847 (2023).
- 16. van Faassen, H. *et al.* Serum albumin-binding VHHs with variable pH sensitivities enable tailored half-life extension of biologics. *The FASEB Journal* **34**, 8155–8171 (2020).
- 17. el Oualid, F. *et al.* Chemical synthesis of ubiquitin, ubiquitin-based probes, and diubiquitin. *Angewandte Chemie International Edition* **49**, 10149–10153 (2010).
- 18. Geurink, P. P. *et al.* Development of Diubiquitin-Based FRET Probes To Quantify Ubiquitin Linkage Specificity of Deubiquitinating Enzymes. *ChemBioChem* **17**, 816–820 (2016).
- 19. Blythe, E. E., Olson, K. C., Chau, V. & Deshaies, R. J. Ubiquitin- A nd ATP-dependent unfoldase activity of P97/VCP•NPLOC4•UFD1L is enhanced by a mutation that causes multisystem proteinopathy. *Proc Natl Acad Sci U S A* **114**, E4380–E4388 (2017).
- 20. Schaft, N., Lankiewicz, B., Gratama, J. W., Bolhuis, R. L. H. & Debets, R. Flexible and sensitive method to functionally validate tumor-specific receptors via activation of NFAT. *J Immunol Methods* **280**, 13–24 (2003).
- 21. Schaft, N. *et al.* Peptide Fine Specificity of Anti-Glycoprotein 100 CTL Is Preserved Following Transfer of Engineered TCR $\alpha\beta$ Genes Into Primary Human T Lymphocytes. *The Journal of Immunology* **170**, 2186–2194 (2003).